Fast Multipole Method Accelerated by Lifting Wavelet Transform Scheme

Ming-Sheng Chen[1], Xian-Liang Wu[1, 2], Wei Sha[3], and Zhi-Xiang Huang [2]

[1] Department of Physics and Electronic Engineering, Hefei Teachers College, 1688 LianHua Road, Economic and Technological Development Zone, Hefei, Anhui 230601, China
cmsh@ahu.edu.cn , xlwu@ahu.edu.cn

[2] Key Laboratory of Intelligent Computing & Signal Processing, Anhui University, Hefei, Anhui 230039, China
zxhuang@ahu.edu.cn

[3] Department of Electrical and Electronic Engineering, the University of Hong Kong, Pokfulam Road, Hong Kong, China
wsha@eee.hku.hk

***Abstract*—** The lifting wavelet like transform (LWLT) is applied to the fast multipole method (FMM) to complete the scattering analysis of three-dimensional (3D) objects. The aggregation matrix and disaggregation matrix are sparsified by the LWLT scheme in time. Numerical results for different shaped three-dimensional objects are considered. It is shown that the proposed method can speed up FMM with lower memory required.

***Index Terms*—** Lifting wavelet like transform (LWLT), Method of moments (MOM), Fast multipole method (FMM), Electromagnetic scattering.

I. INTRODUCTION

As an efficient numerical algorithm for the analysis and computation of electromagnetic scattering by arbitrarily shaped three-dimensional objects, the method of moments (MOM) is widely used in computational electromagnetics (CEM). However, traditional MOM technique is inherently limited because its direct solution has $O(N^3)$ complexity for a problem with N unknowns, and even though the iterative methods are adopted, the matrix-vector multiplication (MVM) can be $O(N^2)$. Over the past few decades, a number of techniques have been proposed to speed up the process of MVM. The fast multipole method (FMM) [1-3] and the multilevel fast multiple algorithm (MLFMA) [4] are well known among them, which can reduce $O(N^2)$ for MVM to $O(N^{1.5})$ and $O(N \log N)$, respectively, and some techniques are proposed to further improve the efficiency. In [5] the Cartesian components of the radiation patterns are represented in a spherical harmonics basis to optimize the memory requirements. Another interesting method is the wavelet matrix method [6-10], which can sparsify the dense moment matrix due to its multiresolution and vanishing moment properties, leading to a reduced solution time for the resulting sparse matrix. The applications of wavelet matrix transform have been widely used but are mainly confined to the analysis of two-dimensional (2-D) problems, or to special structures such as wire in which the current direction is one-dimensional. When 3-D scattering problems are considered, the impedance elements distribution will be more oscillatory than that in 2-D or 1-D cases, and the sparsity obtained by ordinary wavelet can be unsatisfying, which makes the application of wavelet transform to such problems greatly restricted.

II. THEORY

For perfectly electrically conducting (PEC) objects illuminated by an incident field $\mathbf{E}^i(\mathbf{r})$, the electric field integral equation (EFIE) is given by

$$\hat{\mathbf{n}} \times \iint_S \bar{\mathbf{G}}(\mathbf{r},\mathbf{r}') \bullet \mathbf{J}(\mathbf{r}') dS' = \frac{1}{jk\eta} \hat{\mathbf{n}} \times \mathbf{E}^i(\mathbf{r}), \quad (1)$$

where $\mathbf{J}(\mathbf{r}')$ is the unknown current distribution, $\hat{\mathbf{n}}$ is the unit outwardly directed norm vector of surface S, $\bar{\mathbf{G}}(\mathbf{r},\mathbf{r}')$ is the well-known free-space dyadic Green's function given by

$$\bar{\mathbf{G}}(\mathbf{r},\mathbf{r}') = \left(\bar{\mathbf{I}} + \frac{\nabla\nabla}{k^2} \right) g(\mathbf{r},\mathbf{r}'); \; g(\mathbf{r},\mathbf{r}') = \frac{e^{-jk|\mathbf{r}-\mathbf{r}'|}}{4\pi|\mathbf{r}-\mathbf{r}'|}, \quad (2)$$

with $\bar{\mathbf{I}}$ being the unit dyad.

When $\mathbf{J}(\mathbf{r})$ is represented by the Rao-Wilton-Glisson (RWG) basis functions and FMM is applied, equation (1) will be reduced to a matrix equation. For the far groups, the matrix-vector multiplication can be rewritten as

$$\mathbf{Z}^{far}\mathbf{x} = \mathbf{DTAx}, \quad (3)$$

where $\mathbf{x}$ is the unknown current coefficients, and $\mathbf{D}$, $\mathbf{A}$, $\mathbf{T}$ are the disaggregation matrix, aggregation matrix, and translation matrix respectively, which are defined as

$$\mathbf{D}_{mp} = \int_S (\bar{\mathbf{I}} - \hat{\mathbf{k}}_p \hat{\mathbf{k}}_p) \bullet \mathbf{f}_m^S(\mathbf{r}) e^{-j\mathbf{k}_p \bullet (\mathbf{r}-\mathbf{r}_o)} dS, \quad (4)$$

$$\mathbf{A}_{pn} = \int_{S'} (\bar{\mathbf{I}} - \hat{\mathbf{k}}_p \hat{\mathbf{k}}_p) \bullet \mathbf{f}_n^S(\mathbf{r}') e^{j\mathbf{k}_p \bullet (\mathbf{r}'-\mathbf{r}_o')} dS', \quad (5)$$

$$\mathbf{T}_p = \frac{k^2\eta}{16\pi^2} \omega_p \sum_{l=0}^{L} (-j)^l (2l+1) h_l^{(2)}(kX) P_l(\hat{\mathbf{k}}_p \bullet \hat{\mathbf{X}}) \quad p = 1,2,\cdots,2L^2, \quad (6)$$

in which $\mathbf{f}_m^S(\mathbf{r})$ and $\mathbf{f}_n^S(\mathbf{r}')$ are the RWG functions, k is the wavenumber in free space, $\mathbf{r}_o$ and $\mathbf{r}_o'$ are field group center and source group center respectively, $\mathbf{k}_p = k\hat{\mathbf{k}}_p$, $\hat{\mathbf{k}}_p = (\sin\theta_p \cos\phi_p, \sin\theta_p \sin\phi_p, \cos\theta_p)$, (θ_p, ϕ_p) are the sampled points over the unit sphere, X is the center distance between field group and source group, $h_l^{(2)}$(x) is a spherical Hankel function of the second kind, and $P_l(x)$ refers to a Legendre polynomial.

The translation matrix $\mathbf{T}$ is highly sparse and can be further sparsified through the use of a windowed translation operator [12]. In this paper, discussions are focused on the sparsify operations of $\mathbf{D}$ and $\mathbf{A}$. As we know that for the interaction between two far groups, $\mathbf{D}$ is an $M_i \times K$ matrix and $\mathbf{A}$ is a $K \times N_i$ matrix with $K = 2L^2$.

As can be seen from (4) and (5), for a given $\mathbf{f}_m^S(\mathbf{r})$ or $\mathbf{f}_n^S(\mathbf{r}')$, the elements in the corresponding row or column vary with the sampled points on the surface of an unit sphere according to the Gauss-Legendre method. Compared with the elements distribution in traditional impedance matrix for 3-D problem, the elements distribution in $\mathbf{D}$ (row) or $\mathbf{A}$ (column) is relatively regular. That is the reason that the wavelet transform is introduced for the row in $\mathbf{D}$ and the column in $\mathbf{A}$.

The wavelet matrix transformation is applied and the interaction between the two groups can be represented by

$$[\mathbf{D}]_{M_i \times K} [\mathbf{T}]_{K \times K} [\mathbf{A}]_{K \times N_j} \mathbf{x} = [\mathbf{D}]_{M_i \times K} [\mathbf{W}]_{K \times K} [\tilde{\mathbf{W}}]_{K \times K} [\mathbf{T}]_{K \times K} [\mathbf{W}]_{K \times K} [\tilde{\mathbf{W}}]_{K \times K} [\mathbf{A}]_{K \times N_j} \mathbf{x}, \quad (7)$$

where $\tilde{\mathbf{W}}$ and $\mathbf{W}$ are forward and inverse wavelet transform matrices respectively and have the identity $\tilde{\mathbf{W}}\mathbf{W} = \mathbf{I}$, and for orthogonal wavelet $\tilde{\mathbf{W}} = \mathbf{W}^T$.

Equation (7) can be rewritten as

$$\mathbf{DTAx} = \tilde{\mathbf{D}}\tilde{\mathbf{W}}\mathbf{TW}\tilde{\mathbf{A}}\mathbf{x}, \quad (8)$$

with $\tilde{\mathbf{D}} = \mathbf{DW}$ and $\tilde{\mathbf{A}} = \tilde{\mathbf{W}}\mathbf{A}$.

Then the MVM will be completed by the following steps:

- Firstly, $\mathbf{D}$, $\mathbf{A}$ and $\mathbf{T}$ are generated and wavelet matrix transform is applied simultaneity by $\tilde{\mathbf{D}} = \mathbf{DW}$ and $\tilde{\mathbf{A}} = \tilde{\mathbf{W}}\mathbf{A}$, then $\tilde{\mathbf{D}}$ and $\tilde{\mathbf{A}}$ is a sparse matrix by the threshold σ_m.
- Secondly, complete aggregation by $\mathbf{x}_1 = \tilde{\mathbf{A}}\mathbf{x}$, and the inverse wavelet transform for $\mathbf{x}_1$ is implement by $\mathbf{x}_2 = \mathbf{W}\mathbf{x}_1$.
- Thirdly, complete translation by $\mathbf{x}_3 = \mathbf{T}\mathbf{x}_2$.
- Finally, the forward wavelet transform for $\mathbf{x}_3$ is applied by $\mathbf{x}_4 = \tilde{\mathbf{W}}\mathbf{x}_3$, and the disaggregation is completed by $\mathbf{x}_5 = \tilde{\mathbf{D}}\mathbf{x}_4$.

To save CPU time and memory consumed for transform matrix, the lifting wavelet like transform is introduced to complete the forward transform and inverse transform. In the LWLT scheme, the wavelet transform is directly operated to the object matrix according to the polyphase matrices

$$\tilde{\mathbf{P}}(z) = \prod_{i=1}^{m} \begin{pmatrix} 1 & 0 \\ -s_i(z^{-1}) & 1 \end{pmatrix} \begin{pmatrix} 1 & -t_i(z^{-1}) \\ 0 & 1 \end{pmatrix} \begin{pmatrix} F & 0 \\ 0 & 1/F \end{pmatrix}, \quad (9)$$

$$\mathbf{P}(z)=\prod_{i=1}^{m}\begin{pmatrix}1 & s_i(z)\\ 0 & 1\end{pmatrix}\begin{pmatrix}1 & 0\\ t_i(z) & 1\end{pmatrix}\begin{pmatrix}F & 0\\ 0 & 1/F\end{pmatrix}, \quad (10)$$

in which $s_i(z)$ and $t_i(z)$ are Laurent polynomials, and F is a nonzero constant.

The forward transform is implemented according to $\tilde{\mathbf{P}}(z^{-1})^t$ and the inverse transform is operated by $\mathbf{P}(z)$, and specific examples can be found in [11].

For a field group with M_i RWG functions and a source group with N_j RWG functions, there are $2L^2$ elements in each row of **D** or in each column of **A**, and in the presented scheme, the LWLT is actually applied to **D** row by row, and applied to **A** column by column. Take the matrix **D** for example, once a certain row is generated and the transform for it is implemented, then the clipping operation [13] is used with the threshold and only the left elements in the row are stored. The threshold for the m row is defined by

$$\sigma_m=\tau\cdot\frac{1}{K}\sum_{p=1}^{K}\left(\left|\tilde{\mathbf{D}}_\theta(m,p)\right|^2+\left|\tilde{\mathbf{D}}_\varphi(m,p)\right|^2\right)^{\frac{1}{2}}, \quad (11)$$

and numerical simulations show that $\tau\in[0.8,1.2]$, and the accuracy is controlled by τ.

As we can see from the above operations, two wavelet implementations are added to each iterative step. The number of multiplication operations within the LWLT is set to be p which can be counted from the polyphase matrices. If the length of the signal is K, the total computational complexity for implementation LWLT for it can be computed by

$$p\times\frac{K}{2}\times(1+\frac{1}{2}+\frac{1}{4}+...)=pK, \quad (12)$$

and for Daubechies wavelets of 4 vanishing moments (db4) with the maximum level transform $p=12$, which is so smaller than M_i that can be neglected when electrically large problem is considered, since $M_i\approx\sqrt{N}$.

III. NUMERICAL RESULTS

Firstly the disaggregation matrix **D** for a PEC cube is considered with $L=10$. After the lifting wavelet like transform by db4, a row of $\tilde{\mathbf{D}}$ is presented in Figure 1.

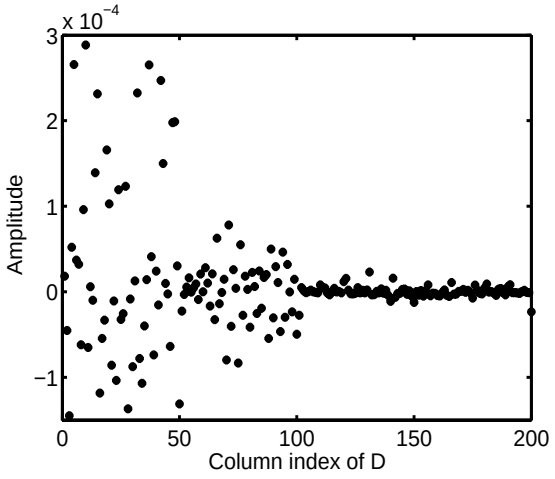

Fig. 1. The elements distribution in disaggregation matrix after the application of LWLT.

As can be seen from Fig. 1, most of the elements are far smaller than the others. The results after the clipping operation is shown in Fig. 2 and only about 30% of the total elements are left, then the inverse LWLT is implemented and the new row after transform is given in Fig. 3 which agrees well with the original row transform in **D**, the relative error is 2.57%, which will ensure the accuracy of MVM computation for far field.

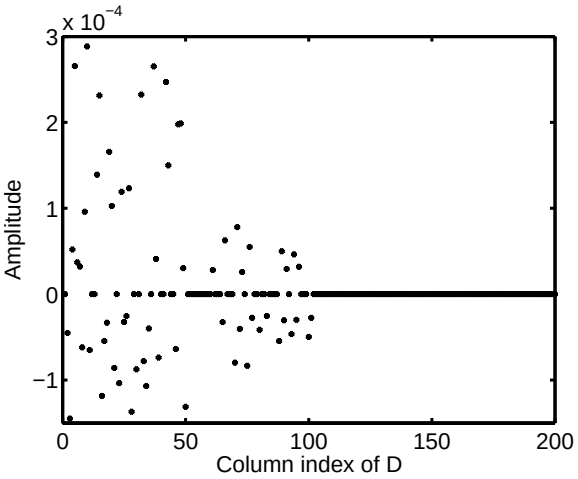

Fig. 2. The elements distribution in disaggregation matrix after the application of clipping technique.

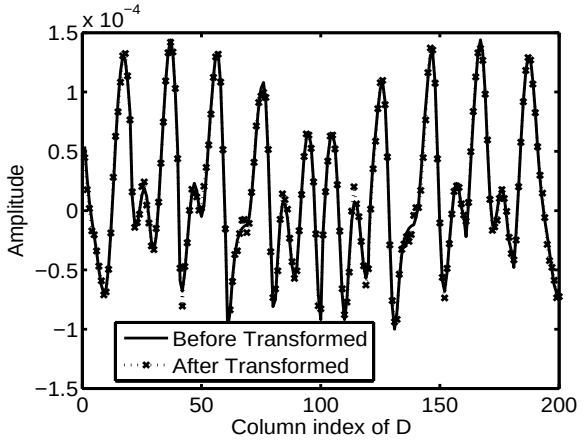

Fig. 3. The elements distribution in disaggregation matrix obtained by inverse lifting wavelet transform from the row presented in Fig. 2, which is compared with the row in $\mathbf{D}$.

As the first example, a PEC sphere with a diameter of 5λ is considered. The total number of unknowns is 15870 and the unknowns are divided into 98 groups with group size $d = 1\lambda$. When the sparsity (defined as the percentage content of nonzero elements) of disaggregation matrix and aggregation matrix is 32.44% ($\tau = 0.9$), the radar cross section (RCS) of the sphere computed by the LWLT-FMM scheme is compared with that of the analytical solution and shown in Fig. 4.

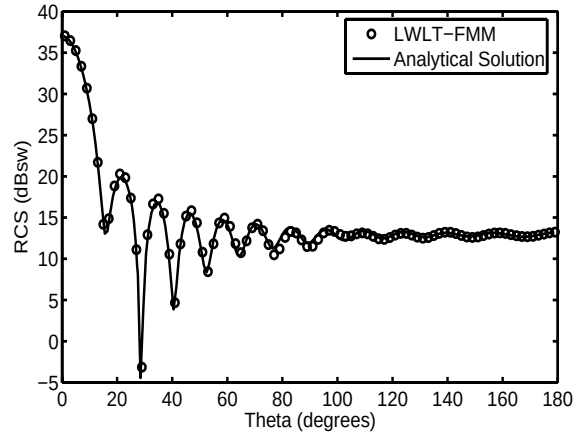

Fig. 4. The E-plane RCS of a PEC sphere with a diameter of 5λ.

A PEC cube with a side length of 4λ is considered as the second example. The surface of it is discretized into 12288 triangular elements, and 98 nonempty boxes are formed with group size $d = 0.8\lambda$. The sparsity of disaggregation matrix and aggregation matrix obtained is 33.13% ($\tau = 1.1$), the LWLT-FMM method obtained the accurate result more quickly as compared with the traditional FMM, which is shown in Fig. 5.

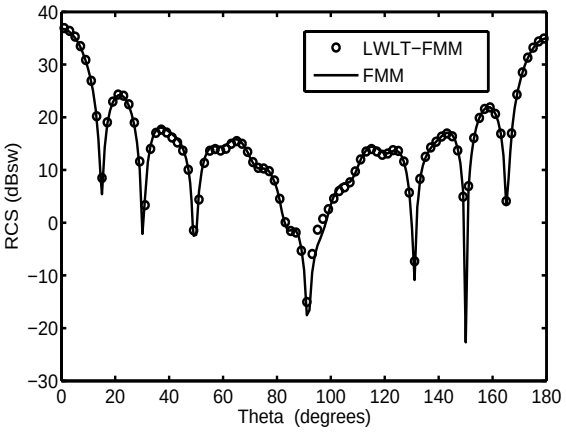

Fig. 5. The E-plane RCS of a PEC cube with a side length of 4λ.

The total CPU time and memory consumed for the MVM in far-field computation is shown in Table I. We can conclude that the proposed method can speed up the FMM by a factor of two with half memory consumed.

Table I The CPU time and memory required for the MVM operations of far-field interactions

Example	CPU time for far field computation		Memory required for Far-field computation	
	FMM	LWLT-FMM	FMM	LWLT-FMM
PEC Sphere $L = 12$	192 seconds	107 seconds	213MB	96MB
PEC Cube $L = 10$	177 seconds	98 seconds	170MB	74MB

IV. DISCUSSION

To validate the effectiveness of the formula presented in equation (11) for the threshold, we define the relative root mean square (RMS) error as

$$Err_{RMS} = \left\{ \frac{1}{M} \sum_{m=1}^{M} \left| 10 \log_{10} \left[\hat{\sigma}(\theta_m) / \sigma(\theta_m) \right] \right|^2 \right\}^{\frac{1}{2}}, \quad (13)$$

where the θ_m represent M selected scattering directions. $\hat{\sigma}$ and σ are the radar cross section obtained by direct FMM solution and LWLT-FMM method, respectively.

For the given two examples mentioned above, the relationship between relative RMS RCS error and the value of parameter τ are shown in Fig.6 and Fig. 7, while the sparsity of disaggregation matrix and aggregation matrix is given in Fig.8, from which we can conclude that the relative RMS RCS error can be controlled under 0.5 dB with the sparsity about 30% when the value of parameter τ is chosen from 0.8 to 1.2.

Finally, when we set $\tau = 0.9$ and $\tau = 1.1$ for the PEC sphere and PEC cube described in the previous section, the nonzero element distribution in disaggregation matrix for the first nonempty box are shown in Fig. 9 and Fig. 10, respectively.

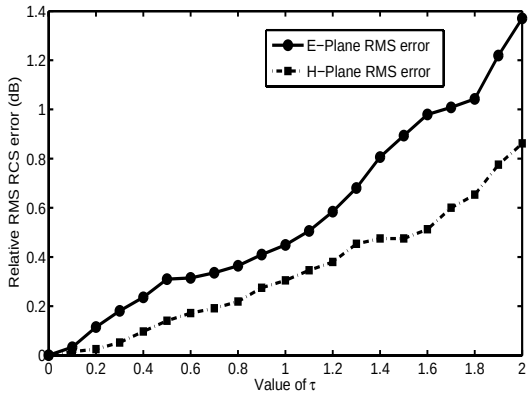

Fig. 6. Relative RMS RCS error of PEC sphere varies with value of τ.

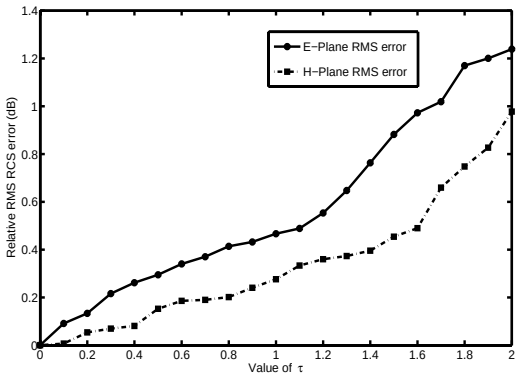

Fig. 7. Relative RMS RCS error of PEC cube varies with value of τ.

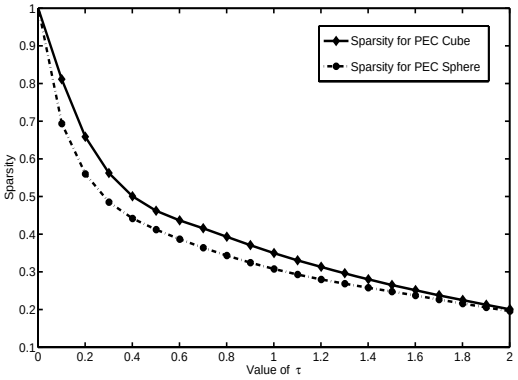

Fig. 8. Sparsity of disaggregation matrix and aggregation matrix varies with value of τ.

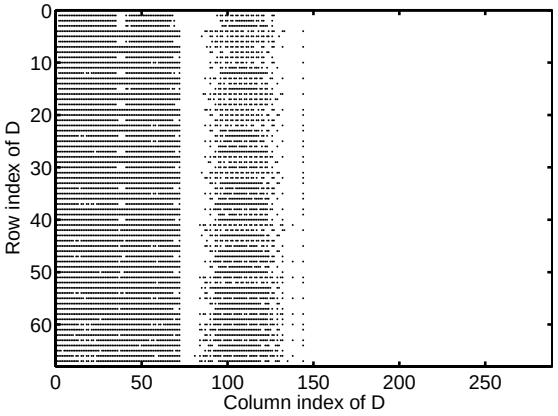

Fig. 9. Nonzero elements distribution for disaggregation matrix of a PEC sphere.

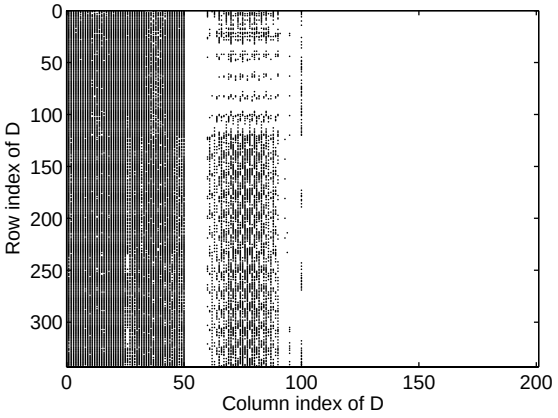

Fig. 10. Nonzero elements distribution for disaggregation matrix of a PEC cube.

V. CONCLUSION

The fast multipole method in conjugation with the LWLT scheme is proposed to the scattering analysis of different shaped three-dimensional PEC objects, the CPU time and memory consumed by FMM are reduced by sparsify the disaggregation matrix and aggregation matrix in time.

ACKNOWLEDGEMENT

The author wishes to acknowledge the anonymous reviewers for their useful comments and constructive suggestions. This work is supported by the Natural Science Foundation of the Anhui Higher Education Institution of China under Grant No KJ2008A036 and partially by the National Natural Science Foundation of China under Grant No 60671051.

REFERENCES

[1] V. Rokhlin, "Rapid solution of integral equations of scattering theory in two dimensions," *J. of Comput. Phys.*, vol. 86, no. 2, pp. 414-439, 1990.

[2] N. Engheta, W. D. Murphy, V. Rokhlin, and M. S. Vassiliou, "The fast multipole method (FMM) for electromagnetic scattering problems," *IEEE Trans. Antennas Propagat*., vol. 40, no. 6, pp. 634-641, 1992.

[3] R.Coifman and V.Rokhlin, "The fast multipole method for the wave equation:a pedestrian prescription," *IEEE Antennas Propagat. Mag.*, vol. 35, no. 3, pp. 7-12, 1993.

[4] J. M. Song and W. C. Chew, "Multilevel fast-multipole algorithm for solving combined field integral equations of electromagnetic scattering," *Micro. Opt. Tech. Lett.,* vol. 10, no. 1, pp. 14-19, 1995.

[5] T. F. Eibert, "A diagonalized multilevel fast multipole method with spherical harmonics expansion of the k-space integrals," *IEEE Trans. Antennas Propag.*, vol. 53, no. 2, pp. 814-817, 2005.

[6] R. L. Wagner and W. C. Chew, "A Study of Wavelets for the Solution of Electromagnetic Integral-Equations," IEEE Transactions on Antennas and Propagation, vol. 43, no. 8, pp. 802-810, 1995.

[7] Z. G. Xiang and Y. L. Lu, "A study of the fast wavelet transform method in computational electromagnetics", *IEEE Trans. Magnetics*, vol. 34, no. 5, pp. 3323-3326, 1998.

[8] H. Deng and H. Ling, "Preconditioning of electromagnetic integral equations using pre-defined wavelet packet basis," *Elect. Lett*., vol. 35, no. 14, pp. 1144-1145, 1999.

[9] J. Yu and A. A. Kishk, "Use of wavelet transform to the method-of-moments matrix arising from electromagnetic scattering problems of 2D objects due to oblique plane-wave incidence," *Micro. Opt. Tech. Lett*., vol. 34, no. 2, pp. 130-134, 2002.

[10] D. Huybrechs and S. Vandewalle, "A two-dimensional wavelet-packet transform for matrix compression of integral equations with highly oscillatory kernel," *J. Comput. App. Math.*, vol. 197, no. 1, pp. 218-232, 2006.

[11] I. Daubechies and W. Sweldens, "Factoring wavelet transforms into lifting steps," *J. of Fourier Analysis and App*., vol. 4, no. 3, pp. 247-269, 1998.

[12] R. L. Wagner, and W. C. Chew, "A ray-propagation fast multipole algorithm," *Micro. Opt. Tech. Lett*., vol. 7, no. 10, pp. 435-438, 1994.

[13] F. P. Andriulli, G. Vecchi, F. Vipiana, P. Pirinoli, and A. Tabacco, "Optimal A priori clipping estimation for wavelet-based method of moments matrices," *IEEE Trans. Antennas Prop*., vol. 53, no. 11, pp. 3726-3734, 2005.

Ming-Sheng Chen was born in Nanling, Anhui Province, China, in 1981. He received the B.S. degree in applied mathematics from Anhui University, Hefei, China, in 2003, and received the Ph.D. degree in electromagnetic scattering, inverse scattering, and target identification at the same university. He is currently working at Department of Physics and Electronic Engineering, Hefei Teachers College. He has authored or coauthored more than 30 papers. His current research interests include frequency-domain numerical methods and wavelet theory.

Xian-Liang Wu was born in Bozhou, Anhui Province, China, in 1955. He received the B.S. degree in electronic engineering from Anhui University, Hefei, China, in 1982. He is a full professor of department of electronic engineering and the director of laboratory of electromagnetic field and microwave technology at Anhui University. He is currently the principal of Hefei Teachers College. He has authored or coauthored more than 70 papers and 2 books. His current research interests include electromagnetic field theory, electromagnetic scattering and inverse scattering, wireless communication, etc.
Prof. Wu is a senior member of Chinese Institute of Electronics, and an associate director of Chinese Institute of Microwave Measurement. He received the "Ministry of Education Award for Science & Technology Progress" and "Science & Technology Award of Anhui Province".

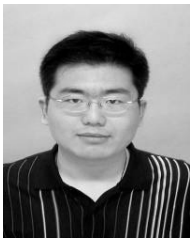

Wei Sha was born in Suzhou, Anhui Province, China, in 1982. He received the B.S. degree in electronic engineering from Anhui University, Hefei, China, in 2003 and received the Ph.D. degree in electromagnetic scattering, inverse scattering, and target identification at the same university. He is currently a postdoctoral research fellow at department of electrical and electronic engineering, the University of Hong Kong. His current research interests include time-domain numerical methods and signal processing.

Zhi-Xiang Huang was born in Guangde, Anhui Province, China, in 1979. He received the B.S. degree in mathematical statistics and the Ph.D. degree in electromagnetic scattering, inverse scattering, and target identification from Anhui University, Hefei, China, in 2002 and 2007, respectively. His current research interests include numerical methods for scattering.